Journal of Pharmaceutical Analysis 11 (2021) 272–277

Contents lists available at ScienceDirect

Journal of Pharmaceutical Analysis

journal homepage: www.elsevier.com/locate/jpa

Original article

Potential treatment with Chinese and Western medicine targeting NSP14 of SARS-CoV-2

Chao Liu [a], Xiaoxiao Zhu [a], Yiyao Lu [a], Xianqin Zhang [a, b], Xu Jia [a, *], Tai Yang [c, **]

[a] Non-coding RNA and Drug Discovery Key Laboratory of Sichuan Province, Chengdu Medical College, Chengdu, Sichuan, 610500, China
[b] Basic Medical School, Chengdu Medical College, Chengdu, Sichuan, 610500, China
[c] School of Pharmacy, Chengdu Medical College, Chengdu, Sichuan, 610500, China

ARTICLE INFO

Article history:
Received 24 March 2020
Received in revised form
2 July 2020
Accepted 6 August 2020
Available online 7 September 2020

Keywords:
SARS-CoV-2
Nonstructural protein 14 (NSP14)
ZINC database
Drug docking

ABSTRACT

The outbreak of coronavirus disease 2019 (COVID-19) caused by severe acute respiratory syndrome coronavirus 2 (SARS-CoV-2) is a serious global health threat. This raises an urgent need for the development of effective drugs against the deadly disease. SARS-CoV-2 non-structural protein 14 (NSP14) carrying RNA cap guanine N7-methyltransferase and 3′-5′ exoribonuclease activities could be a potential drug target for intervention. NSP14 of SARS-CoV-2 shares 98.7% of similarity with the one (PDB 5NFY) of acute respiratory syndrome (SARS) by ClustalW. Then, the SARS-CoV-2 NSP14 structures were modelled by Modeller 9.18 using SARS NSP14 (PDB 5NFY) as template for virtual screening. Based on the docking score from AutoDock Vina1.1.2, 18 small molecule drugs were selected for further evaluation. Based on the 5 ns MD simulation trajectory, binding free energy (ΔG) was calculated by MM/GBSA method. The calculated binding free energies of Saquinavir, Hypericin, Baicalein and Bromocriptine for the *N*-terminus of the homology model were −37.2711 ± 3.2160, −30.1746 ± 3.1914, −23.8953 ± 4.4800, and −34.1350 ± 4.3683 kcal/mol, respectively, while the calculated binding free energies were −60.2757 ± 4.7708, −30.9955 ± 2.9975, −46.3099 ± 3.5689, and −59.8104 ± 3.5389 kcal/mol, respectively, when binding to the C-terminus. Thus, the compounds including Saquinavir, Hypericin, Baicalein and Bromocriptine could bind to the *N*-terminus and C-terminus of the homology model of the SARS-CoV-2 NSP14, providing a candidate drug against SARS-CoV-2 for further study.

1. Introduction

The emergence of severe acute respiratory syndrome coronavirus 2 (SARS-CoV-2) has caused a large global outbreak and is a major public health issue. The high affinity of Spike protein for binding to human ACE2 protein makes SARS-CoV-2 spread rapidly in the population [1,2]. Importantly, the death rate caused by coronavirus disease 2019 (COVID-19) is much higher than the SARS outbreak in 2002–2003 [3]. The World Health Organization (WHO) declared that COVID-19, a pandemic disease caused by SARS-COV-2, has spread to more than 200 countries around the world. However, there is currently no effective drug or vaccine approved to treat COVID-19.

The SARS-CoV-2 genome is a positive-sense, single-stranded mRNA, which contains a 5′-cap structure and a 3′-poly (A) tail [4]. The large replicase polyproteins 1a (pp1a) and pp1b, which are encoded by the 5′-terminal open reading frame 1a/b (ORF1a/b) at the 5′-terminus of the CoV genome, are cleaved by viral proteases to produce non-structural proteins (NSPs) such as RNA-dependent RNA polymerase (RdRp) and helicase (NSP13) [5]. In addition, the non-structural proteins 14 (NSP14) plays an important role in the virus' genome replication and transcription, and it is generally considered as an important functional protein in the coronavirus family [6,7]. NSP14 is a bifunctional enzyme carrying S-adenosyl methionine (SAM) dependent (guanine-N7) N7-methyl transferase (N7-MTase) and 3′–5′ exoribonuclease (ExoN) activities [5,8]. The C-terminal domain N7-MTase activities involved in RNA cap modification, the cap structure at the 5′ end of viral mRNA assists in translation and evading host defense [9]. The *N*-terminal 3′–5′ ExoN plays a proofreading role in the prevention of lethal mutagenesis [5,8], which provides an attractive target for drug design. Computational protein-ligand docking and virtual drug screening

Peer review under responsibility of Xi'an Jiaotong University.
* Corresponding author.
** Corresponding author.
E-mail addresses: jiaxu@cmc.edu.cn (X. Jia), taiyang@cmc.edu.cn (T. Yang).

https://doi.org/10.1016/j.jpha.2020.08.002

could accelerate the discovery of the potential drugs as potential candidates against COVID-19. Compounds based on virtual screening, such as ribavirin, lopinavir and ritonavir, have been shown to inhibit SARS-CoV-2 replication in vitro [10–13]. In this work, the protein homology modeling and molecular docking were performed to select drug candidates targeting NSP14 to treat COVID-19.

2. Materials and methods

2.1. Homology modeling

The SARS-CoV-2 amino acid sequence (Accession number: MN908947) was obtained from database of the National Center for Biotechnology Information (NCBI). The SARS NSP14 amino acid sequence was downloaded from the PDB protein structure database (PDB ID: 5NFY). The homology of above amino acid sequence was aligned using ClustalW and rendered using ESPript version 3.0. Homology model of the target protein was constructed and optimized by Modeller 9.18 using crystal structure of SARS NSP14 (PDB ID: 5NFY) as template. A total of 100 independent structures were constructed, and the one with best DOPE score was selected for further energy minimization by Amber.

2.2. Docking method

The previous study reported that NSP14 crystal structure of SARS is binocular, amino acids 1-287 fold into the ExoN domain, amino acids 301-527 form the N7-MTase domain [8]. In addition, amino acids 288-301 form a complex loop structure connecting ExoN domain and N7-MTase domain. The ExoN domain shares a similar two-metal-ion-assisted mechanism for removal of misincorporated nucleotides [14,15], and the position of Mg^{2+} is also considered to be the active center of exonuclease [8]. Therefore, the docking box was set in a pocket formed by amino acid residues (D90, V91, E191, G189, H188, A187, W186, T277 and D273) around Mg^{2+} (Fig. 1). The docking box of N7-MTase of NSP14 was set where the substrates GpppA and SAM are located (Fig. 1) [8], and the key amino acids were organized in Table S1.

The ligands were downloaded from the ZINC database (FDA, world-not-FDA, investigational-only, http://zinc.docking.org/substances/subsets/). The 2D structure of the compound was then converted into the corresponding 3D coordinates using the Babel server (http://openbabel.sf.net). Then the model was converted to pdbqt format by prepare_receptor4.py script with assigning atom type and partial charge. All rotatable bonds in the ligands were set as flexible for flexible docking. Vina1.1.2 was used for molecular docking.

2.3. Binding free energy calculation

Each simulation system was immersed in a cubic box of TIP3P water with 10 Å distance from the solute. The Na^+ or Cl^- was applied to neutralize the system. General Amber force field (GAFF) 15 and Amber ff14SB force field were used to parameterize the ligand and protein respectively. Altogether 10,000 steps of minimization with constraints (10 kcal/mol/Å^2) on heavy atoms of complex, consisting of 5000 steps of steepest descent minimization and 5000 steps of conjugate gradient minimization, were used to optimize each system. Then each system was heated to 300 K within 0.2 ns, followed by 0.1 ns equilibration in NPT ensemble. Finally, 5 ns MD simulation on each system at 300 K was performed. The minimization, heating and equilibrium were performed with sander program in Amber18. The 5 ns production run was performed with pmemd.cuda. Based on the 5 ns MD simulation trajectory, binding free energy (ΔG) was calculated with MM/GBSA method according to the following equation:

$$\Delta G_{cal} = \Delta H - T\Delta S = \Delta E_{vdw} + \Delta E_{ele} + \Delta G_{gb} + \Delta G_{np} - T\Delta S$$

where ΔE_{ele} and ΔE_{vdw} refer to electrostatic and van der Waals energy terms, respectively, ΔG_{gb} and ΔG_{np} refer to polar and non-polar solvation free energies, respectively. Conformational entropy (TΔS) was not calculated for saving time. Besides, the ligands were compared based on the same target, so it is reasonable to ignore the entropy.

3. Results and discussion

3.1. Sequence and structural analyses

The SARS-nCoV-2 of NSP14 amino acid sequence downloaded from Protein BLAST was very conservative (data not shown). The amino acid sequence alignment revealed that the NSP14 of SARS-CoV-2 shared 98.7% of similarity with the NSP14 (PDB ID: 5NFY) of SARS (Fig. S1), indicating that the results of NSP14 homology modeling would be more reliable. From the 100 homologous structures constructed, the one with the highest DOPE score was selected for the next drug docking. The two active sites of NSP14 were respectively set with two docking pockets (Fig. 1).

3.2. Drug docking and screening

Ten top compounds that showed the lowest negative vina score in a range of −8.6 to −9.7 kcal/mol were selected from the *N*-terminal domain of homology model (Table 1), and eight top compounds with lowest negative vina score in a range of −8.7 to −9.7 kcal/mol were achieved from the C-terminal domain of homology model (Table 2). It was unexpectedly discovered that the four compounds might simultaneously combined the *N*-terminal and C-terminal active centers of the NSP14 simulated structure. These four compounds were Saquinavir, Hypericin, Baicalein and Bromocriptine, respectively.

3.3. Docking results of Saquinavir against SARS-CoV-2 NSP14 model

Saquinavir, as the first FDA-approved human immunodeficiency virus (HIV) protease inhibitor, has been used in the treatment of HIV patients since 1995 [16]. Saquinavir is safe and generally welltolerated in HIV-1-infected adults [17]. Five of the hydrogen bonds involving ASP-273, ASN-252, ASP-90, ALA-187 and LEU-253 were maintained upon the binding of Saquinavir and *N*-terminus of SARS-CoV-2 NSP14 based on our docking results (Fig. 2A). Meanwhile, hydrogen bonds involving ASN-386, GLN-313, GLY-333 and THR-428 maintained upon the binding of Saquinavir and C-terminus of SARS-CoV-2 NSP14 (Fig. 2C). Saquinavir could bind to the *N*- and C-terminal active pockets of the SARS-CoV-2 NSP14 (Figs. 2B and D). The recent study from a drug-target interaction deep learning model showed that Saquinavir can bind to SARS-CoV-2 RNA-dependent RNA polymerase to inhibit the enzyme activity [18]. Our simulation results showed that Saquinavir could bind to two active sites of NSP14; thus Saquinavir could be a candidate drug against SARS-CoV-2 for further research.

3.4. Docking results of Hypericin against SARS-CoV-2 NSP14 model

Hypericin, a main ingredient of traditional Chinese medicine *Hypericum perforatum* L. (St. John's wort), has demonstrated the activity against RNA viruses in vitro by inhibiting viral replication [19]. The present docking results showed that three of the hydrogen

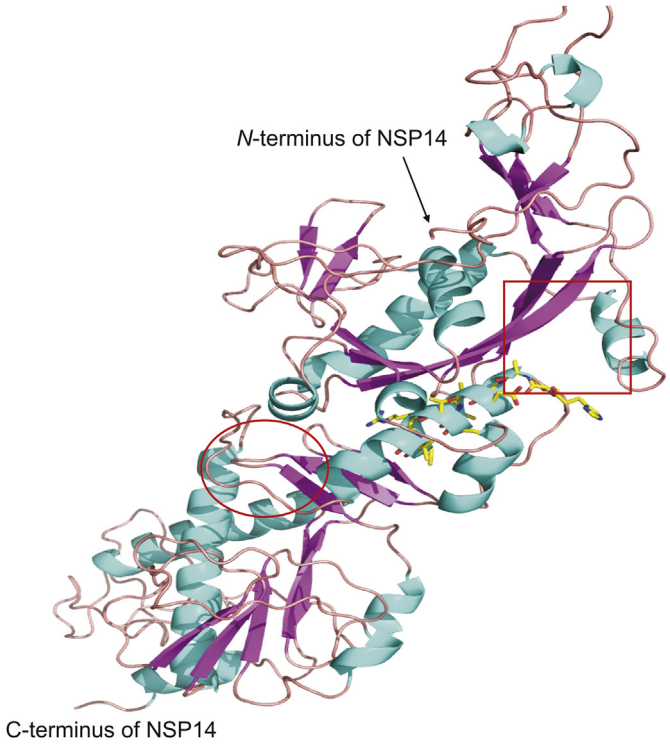

Fig. 1. Cartoon representation of NSP14 homology modeling structure; the active pockets for drug docking are set in red ellipses (C-term) and squares (*N*-term).

bonds involving ASN-252, GLY-93, and HIS-268 were maintained upon the binding of Hypericin and *N*-terminus of SARS-CoV-2 NSP14 (Fig. 3A). The eight hydrogen bonds involving ASN-306 (double), ARG-310 (double), ASN-422, TYR-420 and LYS-336 (double) were maintained upon the binding of Hypericin and C-terminus (Fig. 3C). Hypericin could bind to the *N*- and C-terminal active pockets of the SARS-CoV-2 NSP14 as well (Figs. 2B and D). Hypericin has been proven to have inhibitory effects on human hepatitis C virus (HCV) and human immunodeficiency virus (HIV) [20]. Combined with the present study, Hypericin may have a potential antiviral effect against SARS-CoV-2. Shuanghuanglian oral liquid, composed of *Hypericum perforatum* L, has been widely used for the treatment of viral influenza. However, Shuanghuanglian oral solution suggested for the treatment of SARS-CoV-2 has triggered a huge crisis of public trust among Chinese scientists. We suggested that anti-SARS-CoV-2 effects of Hypericin should be examined in cell culture models with SARS-CoV-2 infection. This will help us have a good understanding of whether it is a good or not to use Chinese medicines for the treatment of SARS-CoV-2.

Table 1
Ten drugs selected from the *N*-terminal domain of homology model.

Drug name	ID	Data	Affinity (kcal/mol)
Hypericin	ZINC000003780340	Investigational-only	−9.7
Bromocriptine	ZINC000053683151	FDA	−9.4
Tanespimycin	ZINC000100014666	Investigational-only	−9.1
Idarubicin	ZINC000003920266	FDA	−9.1
Emend	ZINC000027428713	FDA	−8.9
Baicalein	ZINC000034114798	World-not- FDA	−8.8
Saquinavir	ZINC000029416466	FDA	−8.7
Delavirdine	ZINC000018516586	FDA	−8.7
Silibinin	ZINC000001530850	Investigational-only	−8.6
Golvatinib	ZINC000043195317	Investigational-only	−8.6

3.5. Docking results of Baicalein against SARS-CoV-2 NSP14 model

Baicalein, a flavonoid compound isolated from the root of *Scutellaria baicalensis Georgi* (Huang Qin in Chinese), inhibits viral replication of parainfluenza, influenza A, hepatitis B, HIV-1, and SARS coronavirus [21–23]. The present docking results showed that seven of the hydrogen bonds involving ASN-266, ASN-252, ASP-273, GLY-93, GLU-92 and HIS-268 (double) were maintained upon the binding of Baicalein and *N*-terminus of SARS-CoV-2 NSP14 (Fig. 4A). Five hydrogen bonds involving ASN-386 (double), ASP-331 (double), and GLN-313 were maintained upon the binding of Baicalein and C-terminus (Fig. 4C). Baicalein could also bind to the *N*- and C-terminal active pockets of the SARS-CoV-2 NSP14 (Figs. 4B and D). The previous study showed that Baicalein as a novel chemical inhibitor could inhibit ATPase activity of NSP13 protein of SARS coronavirus [24]. The present data suggested that Baicalein may bind to NSP14 protein to exert anti-SARS-CoV-2 activity. Therefore, we suspect that the anti-SARS-CoV-2 activity induced by Baicalein could be valuable for further study.

3.6. Docking results of Bromocriptine against SARS-CoV-2 NSP14 model

Bromocriptine, a specific dopamine receptor agonist for the hypothalamus and pituitary, has an inhibitory effect on replication of the Dengue virus with low cytotoxicity (half maximal effective concentration, EC_{50} = 0.8–1.6 μM; and half maximal cytotoxicity concentration, CC_{50} = 53.6 μM) [25]. Moreover, Bromocriptine inhibited Zika virus protease activities and exhibited synergistic effects with interferon-α2b against Zika virus replications [26]. It is interesting that Bromocriptine could bind to the *N*- and C-terminal active pockets of the SARS-CoV-2 NSP14 (Figs. 5B and D). Three of the hydrogen bonds involving ASN-104, ASP-273 and GLN-145 were maintained upon the binding of Bromocriptine and *N*-terminus of SARS-CoV-2 NSP14 (Fig. 5A). There was one bond involving THR-428 maintained upon the binding of Bromocriptine and C-terminus of it (Fig. 5C).

3.7. Binding free energy

The Table S2 indicates that Saquinavir, Hypericin, Baicalein and Bromocriptine interact with key amino acid in the active center of NSP14. Based on the 5 ns MD simulation trajectory, ΔG was calculated by MM/GBSA method. The calculated binding free energies of Saquinavir, Hypericin, Baicalein and Bromocriptine for the *N*-terminus of the homology model were −37.2711 ± 3.2160, −30.1746 ± 3.1914, −23.8953 ± 4.4800, and −34.1350 ± 4.3683 kcal/mol, respectively (Table 3), while the calculated binding free energies were −60.2757 ± 4.7708, −30.9955 ± 2.9975, −46.3099 ± 3.5689, and −59.8104 ± 3.5389 kcal/mol, respectively, when binding to the C-terminus (Table 4). Taken together, the results demonstrated that Saquinavir had a strong binding free energy.

Table 2
Eight drugs selected from the C-terminal domain of homology model.

Drug name	ID	Data	Affinity (kcal/mol)
Hypericin	ZINC000003780340	Investigational-only	−9.7
Olysio	ZINC000164760756	FDA	−9.4
Sovaprevir	ZINC000085537149	Investigational-only	−9.1
Celsentri	ZINC000003817234	FDA	−9.1
Saquinavir	ZINC000003914596	FDA	−8.9
Maraviroc	ZINC000101160855	World-not-FDA	−8.8
Baicalein	ZINC000034114798	World-not- FDA	−8.7
Bromocriptine	ZINC000053683151	FDA	−8.7

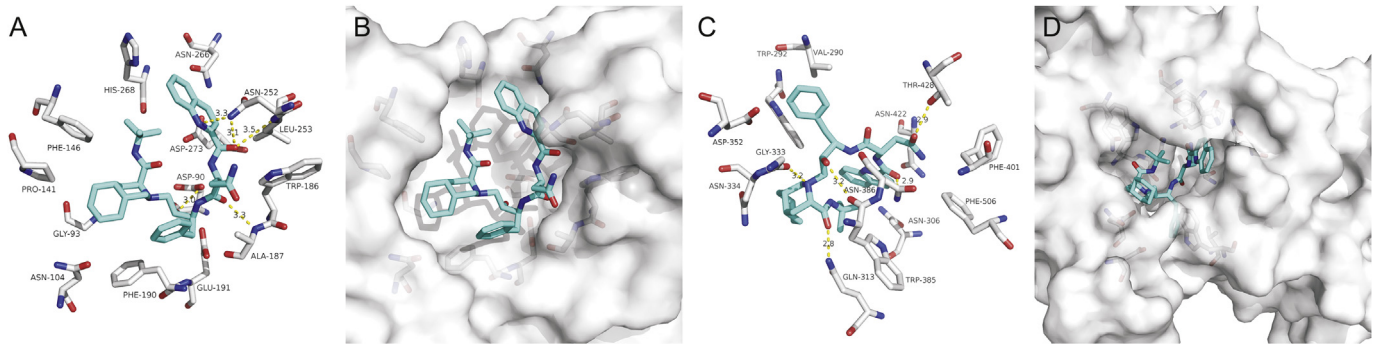

Fig. 2. The binding model of Saquinavir against SARS-CoV-2 NSP14. (A) Interactions between Saquinavir (cyan) and associated residues (off-white) in the *N*-terminus of the homology model for SARS-CoV-2; (B) Binding models of Saquinavir (cyan) in the SARS-CoV-2 NSP14 protein *N*-terminus pocket (white surface); (C) Interactions between Saquinavir (cyan) and associated residues (off-white) in the C-terminus of the homology model for SARS-CoV-2; (D) Binding models of Saquinavir (cyan) in the SARS-CoV-2 NSP14 protein C-terminus pocket (white surface). Numbers accompanying dashed yellow lines represent the interaction distance (Å).

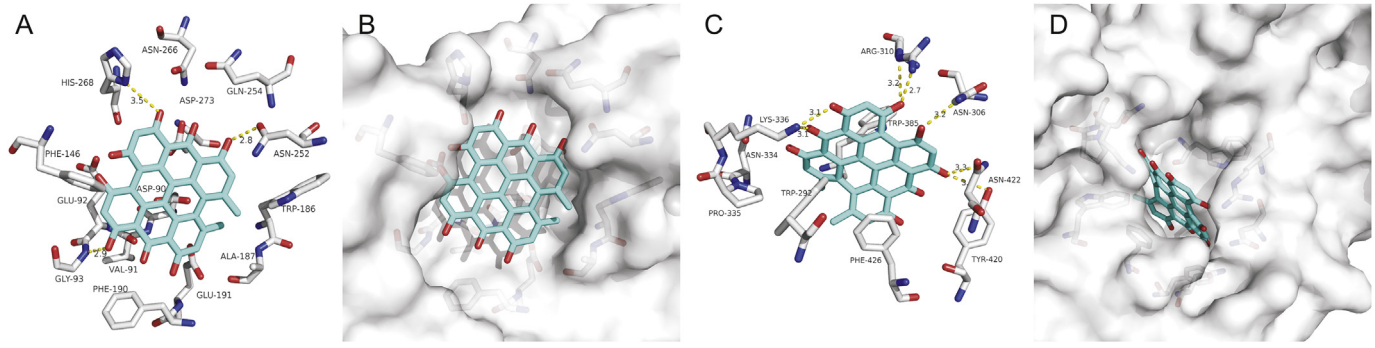

Fig. 3. The binding model of Hypericin against SARS-CoV-2 NSP14. (A) Interactions between Hypericin (cyan) and associated residues (off-white) in the *N*-terminus of the homology model for SARS-CoV-2; (B) Binding models of Hypericin (cyan) in the SARS-CoV-2 NSP14 protein *N*-terminus pocket (white surface); (C) Interactions between Hypericin (cyan) and associated residues (off-white) in the C-terminus of the homology model for SARS-CoV-2; (D) Binding models of Hypericin (cyan) in the SARS-CoV-2 NSP14 protein C-terminus pocket (white surface). Numbers accompanying dashed yellow lines represent the interaction distance (Å).

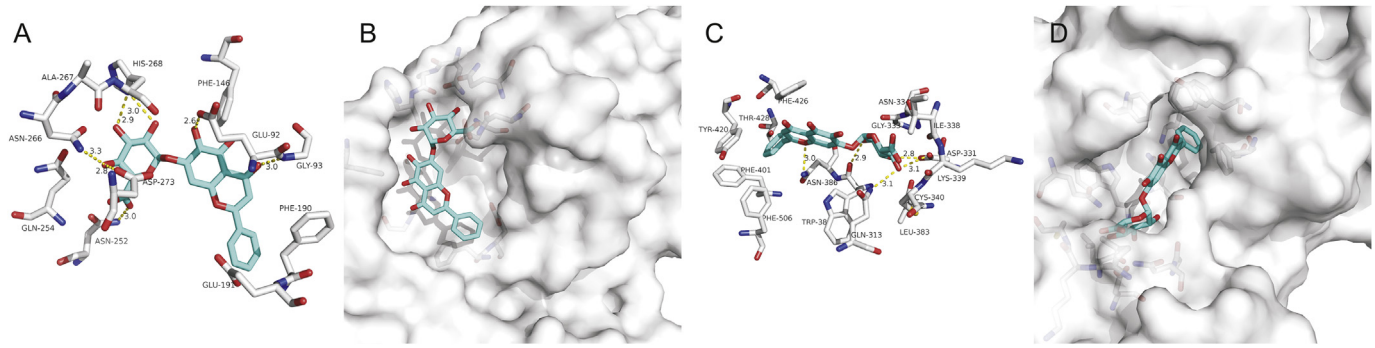

Fig. 4. The binding model of Baicalein against SARS-CoV-2 NSP14. (A) Interactions between Baicalein (cyan) and associated residues (off-white) in the *N*-terminus of the homology model for SARS-CoV-2; (B) Binding models of Baicalein (cyan) in the SARS-CoV-2 NSP14 protein *N*-terminus pocket (white surface); (C) Interactions between Baicalein (cyan) and associated residues (off-white) in the C-terminus of the homology model for SARS-CoV-2; (D) Binding models of Baicalein (cyan) in the SARS-CoV-2 NSP14 protein C-terminus pocket (white surface). Numbers accompanying dashed yellow lines represent the interaction distance (Å).

4. Conclusion

SARS-CoV-2 NSP14, a bifunctional enzyme carrying RNA cap guanine N7-methyltransferase and 3′-5′ exoribonuclease activities, could be a potential drug target for intervention. SARS-CoV-2 NSP 14 shares 98.7% of sequence similarity with the corresponding one in SARS. Thus, the homology model of SARS-CoV-2 NSP14 was structured for virtual screening. Based on the docking score, 18 drugs were selected for further evaluation. Four drugs (Saquinavir, Hypericin, Baicalein and Bromocriptine) could bind to the *N*-terminal and C-terminal domains of SARS-CoV-2 NSP 14, and these drugs all interacted with key amino acid residues in the active center. We suggest the anti-SARS-CoV-2 effects of the above four drugs should be evaluated in the cell culture models with SARS-CoV-2 infection.

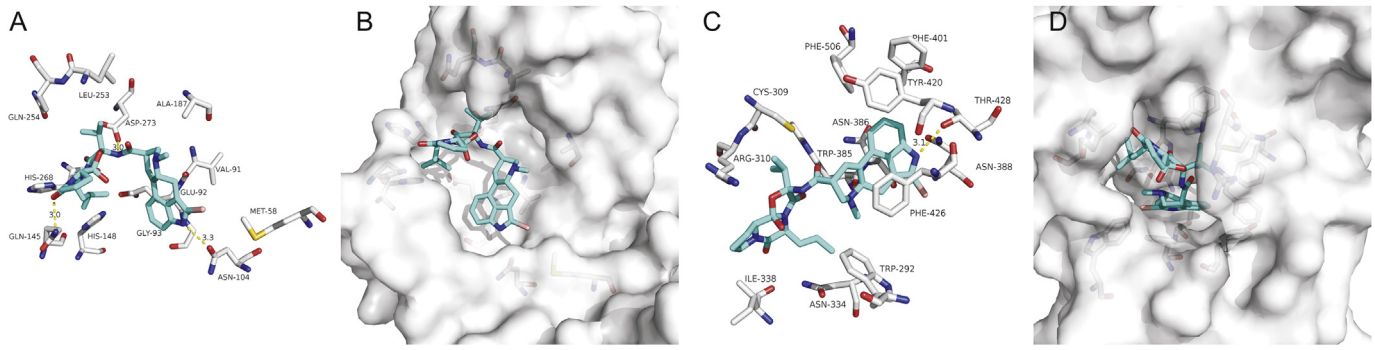

Fig. 5. The binding model of Bromocriptine against SARS-CoV-2 NSP14. (A) Interactions between Bromocriptine (cyan) and associated residues (off-white) in the *N*-terminus of the homology model for SARS-CoV-2; (B) Binding models of Bromocriptine (cyan) in the SARS-CoV-2 NSP14 protein *N*-terminus pocket (white surface); (C) Interactions between Bromocriptine (cyan) and associated residues (off-white) in the C-terminus of the homology model for SARS-CoV-2; (D) Binding models of Bromocriptine (cyan) in the SARS-CoV-2 NSP14 protein C-terminus pocket (white surface). Numbers accompanying dashed yellow lines represent the interaction distance (Å).

Table 3
The calculated binding energies of ligand to the *N*-terminus of SARS-CoV-2 NSP14.

Energy[a]	Saquinavir	Hypericin	Baicalein	Bromocriptine
ΔE_{vdw}	−52.9602 ± 2.9999	−36.4737 ± 4.0922	−36.8721 ± 3.4155	−45.8461 ± 3.1764
ΔE_{ele}	−128.6886 ± 21.2732	−78.5578 ± 10.7496	−47.8615 ± 12.4900	−119.9028 ± 8.3707
ΔG_{gb}	151.4060 ± 21.5835	90.4227 ± 7.8130	66.0255 ± 11.0420	137.3970 ± 6.4239
ΔG_{np}	−7.0283 ± 0.3128	−5.5659 ± 0.2085	−5.1872 ± 0.2001	−5.7839 ± 0.2553
ΔG_{cal}	−37.2711 ± 3.2160	−30.1746 ± 3.1914	−23.8953 ± 4.4800	−34.1350 ± 4.3683

[a] ΔE_{vdw} = van der Waals energy terms; ΔE_{ele} = electrostatic energy; ΔG_{gb} = polar solvation free energy; ΔG_{np} = nonpolar solvation free energy; ΔG_{cal} = final estimated binding free energy calculated from the above terms (kcal/mol).

Table 4
The calculated binding energies of ligand to the C-terminus of SARS-CoV-2 NSP14.

Energy[a]	Saquinavir	Hypericin	Baicalein	Bromocriptine
ΔE_{vdw}	−70.4383 ± 4.1035	−45.7290 ± 2.4822	−48.6473 ± 3.5522	−61.4659 ± 2.9431
ΔE_{ele}	−38.8487 ± 7.5603	−58.4555 ± 12.1238	−192.8463 ± 18.1708	−62.3583 ± 7.0875
ΔG_{gb}	57.7780 ± 6.3018	78.5444 ± 10.3832	202.1598 ± 16.7035	70.6739 ± 5.6693
ΔG_{np}	−8.7666 ± 0.3476	−5.3546 ± 0.2317	−6.9761 ± 0.1614	−6.6602 ± 0.2480
ΔG_{cal}	−60.2757 ± 4.7708	−30.9955 ± 2.9975	−46.3099 ± 3.5689	−59.8104 ± 3.5389

[a] ΔE_{vdw} = van der Waals energy terms; ΔE_{ele} = electrostatic energy; ΔG_{gb} = polar solvation free energy; ΔG_{np} = nonpolar solvation free energy; ΔG_{cal} = final estimated binding free energy calculated from the above terms (kcal/mol).

Declaration of competing interest

The authors declare that there are no conflicts of interest.

Acknowledgments

This work was supported by grants from the National Natural Science Foundation of China (Grant Nos. 31870135, 31600116) and the “1000 Talent Plan” of Sichuan Province (No. 980).

Appendix A. Supplementary data

Supplementary data to this article can be found online at https://doi.org/10.1016/j.jpha.2020.08.002.

References

[1] D. Wrapp, N. Wang, K.S. Corbett, et al., Cryo-EM structure of the 2019-nCoV spike in the prefusion conformation, Science 367 (2020) 1260–1263.
[2] S. Xia, M. Liu, C. Wang, et al., Inhibition of SARS-CoV-2 (previously 2019-nCoV) infection by a highly potent pan-coronavirus fusion inhibitor targeting its spike protein that harbors a high capacity to mediate membrane fusion, Cell Res. 30 (2020) 343–355.
[3] A.A. Rabaan, S.H. Al-Ahmed, S. Haque, et al., SARS-CoV-2, SARS-CoV, and MERS-COV: a comparative overview, Inf. Med. 28 (2020) 174–184.
[4] N. Zhu, D. Zhang, W. Wang, et al., A novel coronavirus from patients with pneumonia in China, 2019, N. Engl. J. Med. 382 (2020) 727–733.
[5] F. Ferron, L. Subissi, A.T. Silveira De Morais, et al., Structural and molecular basis of mismatch correction and ribavirin excision from coronavirus RNA, Proc. Natl. Acad. Sci. U. S. A. 115 (2018) E162–E171.
[6] E.J. Snijder, E. Decroly, J. Ziebuhr, The nonstructural proteins directing coronavirus RNA synthesis and processing, Adv. Virus Res. 96 (2016) 59–126.
[7] I. Sola, F. Almazán, S. Zúñiga, et al., Continuous and discontinuous RNA synthesis in coronaviruses, Annu. Rev. Virol. 2 (2015) 265–288.
[8] Y. Ma, L. Wu, N. Shaw, et al., Structural basis and functional analysis of the SARS coronavirus nsp14-nsp10 complex, Proc. Natl. Acad. Sci. U. S. A. 112 (2015) 9436–9441.
[9] E. Decroly, F. Ferron, J. Lescar, B. Canard, Conventional and unconventional mechanisms for capping viral mRNA, Nat. Rev. Microbiol. 10 (2011) 51–65.
[10] L.I.D.S. Hage-Melim, L.B. Federico, N.K.S. de Oliveira, et al., Virtual screening, ADME/Tox predictions and the drug repurposing concept for future use of old drugs against the COVID-19, Life Sci. 256 (2020), 117963.
[11] S. Pant, M. Singh, V. Ravichandiran, U.S.N. Murty, H.K. Srivastava, Peptide-like and small-molecule inhibitors against Covid-19, J. Biomol. Struct. Dyn. 39 (2020), 2904–2913.
[12] K.T. Choy, A.Y. Wong, P. Kaewpreedee, et al., Remdesivir, lopinavir, emetine, and homoharringtonine inhibit SARS-CoV-2 replication in vitro, Antivir. Res. 178 (2020), 104786.
[13] S.S. Jean, P.I. Lee, P.R. Hsueh, Treatment options for COVID-19: the reality and challenges, J. Microbiol. Immunol. Infect. 53 (2020) 436–443.
[14] P. Chen, M. Jiang, T. Hu, et al., Biochemical characterization of exoribonuclease encoded by SARS coronavirus, J. Biochem. Mol. Biol. 40 (2007) 649–655.
[15] S. Hamdan, P.D. Carr, S.E. Brown, et al., Structural basis for proofreading

during replication of the *Escherichia coli* chromosome, Structure 10 (2002) 535–546.
[16] V.S. Kitchen, C. Skinner, K. Ariyoshi, et al., Safety and activity of saquinavir in HIV infection, Lancet 345 (1995) 952–955.
[17] C.J. la Porte, Saquinavir, the pioneer antiretroviral protease inhibitor, Expet. Opin. Drug Metabol. Toxicol. 5 (2009) 1313–1322.
[18] B.R. Beck, B. Shin, Y. Choi, et al., Predicting commercially available antiviral drugs that may act on the novel coronavirus (SARS-CoV-2) through a drug-target interaction deep learning model, Comput. Struct. Biotechnol. J. 18 (2020) 784–790.
[19] A. Karioti, A.R. Bilia, Hypericins as potential leads for new therapeutics, Int. J. Mol. Sci. 11 (2010) 562–594.
[20] J. Lenard, A. Rabson, R. Vanderoef, Photodynamic inactivation of infectivity of human immunodeficiency virus and other enveloped viruses using hypericin and rose bengal: inhibition of fusion and syncytia formation, Proc. Natl. Acad. Sci. U. S. A. 90 (1993) 158–162.
[21] G.H. Zhang, Q. Wang, J.J. Chen, et al., The anti-HIV-1 effect of scutellarin, Biochem. Biophys. Res. Commun. 334 (2005) 812–816.
[22] P. Sithisarn, M. Michaelis, M. Schubert-Zsilavecz, et al., Differential antiviral and anti-inflammatory mechanisms of the flavonoids biochanin A and baicalein in H5N1 influenza A virus-infected cells, Antivir. Res. 97 (2013) 41–48.
[23] M.J. Hour, S.H. Huang, C.Y. Chang, et al., Baicalein, ethyl acetate, and chloroform extracts of Scutellaria baicalensis inhibit the neuraminidase activity of pandemic 2009 H1N1 and seasonal influenza A viruses, Evid. Based Complement Alternat. Med. 2013 (2013), 750803.
[24] Y.S. Keum, J.M. Lee, M.S. Yu, et al., Inhibition of SARS coronavirus helicase by baicalein, Bull. Kor. Chem. Soc. 34 (2013) 3187–3188.
[25] F. Kato, Y. Ishida, S. Oishi, et al., Novel antiviral activity of bromocriptine against dengue virus replication, Antivir. Res. 131 (2016) 141–147.
[26] J.F. Chan, K.K. Chik, S. Yuan, et al., Novel antiviral activity and mechanism of bromocriptine as a Zika virus NS2B-NS_3 protease inhibitor, Antivir. Res. 141 (2017) 29–37.